Available online at www.sciencedirect.com
ScienceDirect
Journal of Catalysis 251 (2007) 123–130
JOURNAL OF CATALYSIS
www.elsevier.com/locate/jcat

Hydrogenation of 1,3-butadiene on Pd(111) and PdSn/Pd(111) surface alloys under UHV conditions

Christian Breinlich [a], Jan Haubrich [a], Conrad Becker [a,*], Ana Valcárcel [b], Françoise Delbecq [b], Klaus Wandelt [a]

[a] *Institut für Physikalische und Theoretische Chemie der Universität Bonn, Wegelerstr. 12, 53115 Bonn, Germany*
[b] *Laboratoire de Chimie, UMR CNRS 5182, Ecole Normale Supérieure de Lyon, 46 Allée d'Italie, 69364 Lyon Cedex 07, France*

Received 16 April 2007; revised 26 June 2007; accepted 3 July 2007

Available online 21 August 2007

Abstract

The hydrogenation of butadiene on Pd(111) and PdSn/Pd(111) surfaces was investigated by TPD, HREELS, AES, LEED, and UPS. On Pd(111), hydrogenation to butanes, as well as decomposition to surface carbon, which cokes the catalyst, were observed. Formation of butane was not detected. Using a combination of HREELS and DFT, a tetra-σ adsorption mode for butadiene was found. Annealing of thin Sn film on Pd(111) at different temperatures led to the formation of PdSn surface alloys, two of which—Pd_3Sn/Pd(111) and Pd_2Sn/Pd(111)—are ordered structures with $p(2\times 2)$ and $(\sqrt{3}\times\sqrt{3})R30^\circ$ superstructures, respectively. Six different surface alloys were investigated by TPD; it was found that the reactivity, adsorption energy, and branching ratio for hydrogenation/decomposition changed with increasing tin content. HREELS spectra on the Pd_2Sn/Pd(111) alloy revealed a smaller double-bond activation than on Pd(111). The results on the PdSn/Pd(111) surface alloys, in combination with data for the corresponding PtSn/Pt(111) systems, demonstrated general patterns for the hydrogenation reaction of butadiene on noble metal surfaces.

Keywords: Hydrogenation; Butadiene; Temperature-programmed desorption (TPD); High-resolution electron energy loss spectroscopy (HREELS); Palladium; Tin; Alloys

1. Introduction

Since the early work of Bond et al. [1] and Wells et al. [2,3], the selective hydrogenation of butadiene has received much attention, because butadiene is an ideal molecule for use in studying both the activity and selectivity of catalysts. The surface science approach toward catalysis uses simple model systems to establish correlations among adsorption modes, bond activation, and reactivity of a molecule. Because Pt and Pd show the highest activity for butadiene hydrogenation, several studies have focused on either reactivity studies under elevated pressure [4–7] or surface science studies under ultrahigh vacuum (UHV) conditions [8–13] on the two metals to gain insight into the adsorption modes and reaction mechanisms. In general, it has been found that Pd has a higher activity and selectivity for hydrogenation than Pt. Furthermore, (110) facets have a higher activity than (111) facets. The difference between Pd and Pt has been explained in terms of the different adsorption modes and energies. According to NEXAFS measurements, butadiene adsorbs in a di-σ mode on Pt(111) and in a di-π mode on Pd(111) [9,10], whereas EELS measurements indicate a combination of di-σ and tetra-σ modes on Pt(111) [8]. In contrast, theoretical studies postulate a tetra-σ mode as the most stable form on both surfaces [14,15]. Furthermore, a recent theoretical study [16] pointed out that rather than the adsorption modes of the reactants and products, the ability of the surface to stabilize an energetically favored transition state determines the activity and selectivity of a surface.

Zhao and Koel [17,18] and Jugnet et al. [19] extended the research from Pt(111) to bimetallic systems by alloying Pt surfaces with Sn. This reduces the activity but increases the selectivity toward butenes under reaction conditions. In contrast

* Corresponding author.
E-mail address: conrad.becker@uni-bonn.de (C. Becker).

0021-9517/$ – see front matter
doi:10.1016/j.jcat.2007.07.003

to Pt(111), which decomposes butadiene under UHV conditions, it is possible to hydrogenate butadiene to butenes on PdSn alloys in UHV. Many studies have focused only on the selectivity toward formation of different butenes and butane, neglecting the importance of the decomposition pathway, which leads to carbon deposition and coking and thus deactivation of the catalyst. In this work, we present experimental and theoretical data on the adsorption and decomposition of butadiene on Pd(111) and SnPd surface alloys. With the aid of Auger electron spectroscopy (AES), temperature-programmed desorption (TPD), and high-resolution electron energy loss spectroscopy (HREELS), the influence of surface composition on the adsorption mode, reactivity, and selectivity toward butene, butane, and coke formation can be elucidated. Because previous studies [20,21] have shown that alloying with tin can improve the carbon coking properties of metal catalysts, we focus especially on coke formation, because it leads to catalyst poisoning and reduced catalyst lifetime.

2. Experimental

All experiments were conducted in two UHV chambers, both operating at a base pressure of 1×10^{-8} Pa, which have been described previously [25]. These chambers were equipped with an argon sputtering gun, AES, LEED, a quadrupole mass spectrometer (QMS) for TPD experiments, and liquid nitrogen sample cooling. One chamber hosts an angle-integrating UP spectrometer working with He I and He II radiation and an energy resolution of 0.25 eV. The angle of incidence of the photons is 45° off the surface normal. The other chamber contains an Ibach-type HREEL spectrometer operated at 5 eV primary energy and a typical resolution of 3.5–4 meV. All spectra were recorded in specular geometry.

Tin was evaporated from a directly heated Knudsen cell heated to 1080 K. Gases were dosed through leak valves with exposures measured in Langmuirs ($1\ \mathrm{L} = 1.33 \times 10^{-4}$ Pa s). Butadiene was obtained from Fluka with a purity of 99.5%. The Pd(111) sample was cleaned by repeated cycles of Ar^+ sputtering at 900 K (1 kV, ~3 μA sample current), followed by annealing at 1050 K. From time to time, the sample was heated to 800 K in 10^{-3} Pa of oxygen to remove surface carbon. The sample cleanliness was verified by AES, LEED, and HREELS. To remove the deposited tin, the sample was first sputtered at room temperature to prevent large quantities of tin from diffusing into the bulk.

Theoretical calculations were done by DFT using the VASP package. The HREELS spectra were simulated by calculation of the vibrational frequencies. This technique is based on the numerical calculation of the second derivatives of the potential energy surface within the harmonic approach. The force constant matrix is built with finite differences of the first derivatives of the total energy by geometrical perturbations of the optimized Cartesian coordinates of the system. The diagonalization of this matrix provides the harmonic molecular frequencies and the associated harmonic normal vibration modes. The intensities of the EELS spectra are estimated by applying formula (1), in which the intensities are proportional to the square of the dynamic dipole moments (first derivative of the dipole moments with respect to each normal mode), to a function depending on experimental parameters, and to the inverse of the frequencies. Note that only the vibrational modes that lead to an oscillating dipolar moment perpendicular to the surface are active (metal surface selection rule [MSSR]):

$$\frac{I^{\mathrm{k}}_{\mathrm{loss}}}{I_{\mathrm{elastic}}} = \left(\sum_{i=1}^{3N} \frac{P_{\mathrm{k}i}}{\sqrt{m_i}} \frac{\mathrm{d}\mu_z}{\mathrm{d}\Delta r_i} \right)^2 \frac{F(\omega_{\mathrm{k}})}{\omega_{\mathrm{k}}} n_{\mathrm{s}} \tag{1}$$

Further computational details are available elsewhere [14].

3. Hydrogenation of butadiene on Pd(111)

Fig. 1 shows a TPD and a HREELS series for butadiene adsorbed on Pd(111). Masses of $m/e = 54$ for butadiene, $m/e = 56$ for butene, and $m/e = 58$ for butane were recorded by TPD ($\beta = 3$ K/s) after adsorption of 4 L hydrogen and 6 L butadiene at 90 K. Clearly, butadiene can be hydrogenated under UHV conditions, because butene desorption is observed in a symmetric peak centered around 230 K. Butadiene does not desorb from the monolayers, indicating a total conversion of the adsorbed butadiene. The butadiene desorption peak at 120 K corresponds to multilayer desorption; a Redhead [22] approximation yields a desorption energy for this multilayer of 32 kJ/mol, which is close to the evaporation enthalpy of butadiene. There is no indication for the formation of butane.

The series of HREELS spectra supports these results. The spectrum recorded at 100 K corresponds to the physisorbed multilayer, which is very similar to condensed phase infrared spectra of butadiene. From 160 to 300 K, a characteristic loss pattern can be seen that corresponds to chemisorbed butadiene in the monolayer. In this temperature range, only intensities changes with increasing temperature are observed in the HREELS spectra. At higher temperatures, the spectra become less structured, indicating the formation of the dehydrogenated hydrocarbon fragments, which arise from decomposition of remaining parts of the butadiene monolayer. Finally, surface carbon is formed (750 K), which cokes the catalyst. Subsequent reaction cycles without preparation of a new sample show a strongly reduced activity of the surface due to this coking. Because the spectral pattern of the monolayer does not change within the temperature interval in which hydrogenation occurs, we conclude that the butene desorption is a reaction-limited process. The peak observed at 1800 cm^{-1} in the 750 K spectrum can be attributed to co-adsorbed CO stemming from the sample heating, which has been adsorbed during cooling of the sample. The HREELS series agrees nicely with a recent study conducted by Silvestre-Albero et al. [13], who performed a temperature-dependent XPS investigation showing multilayer desorption at 120 K and butadiene decomposition at temperatures above 500 K.

Fig. 2 shows a comparison of the 160 K monolayer experimental HREELS spectrum with the calculated spectra of the tetra-σ and the di-σ-3,4-π adsorption modes. The theoretical spectrum of the tetra-σ mode, which corresponds to the adsorption geometry from Ref. [14], is in excellent agreement

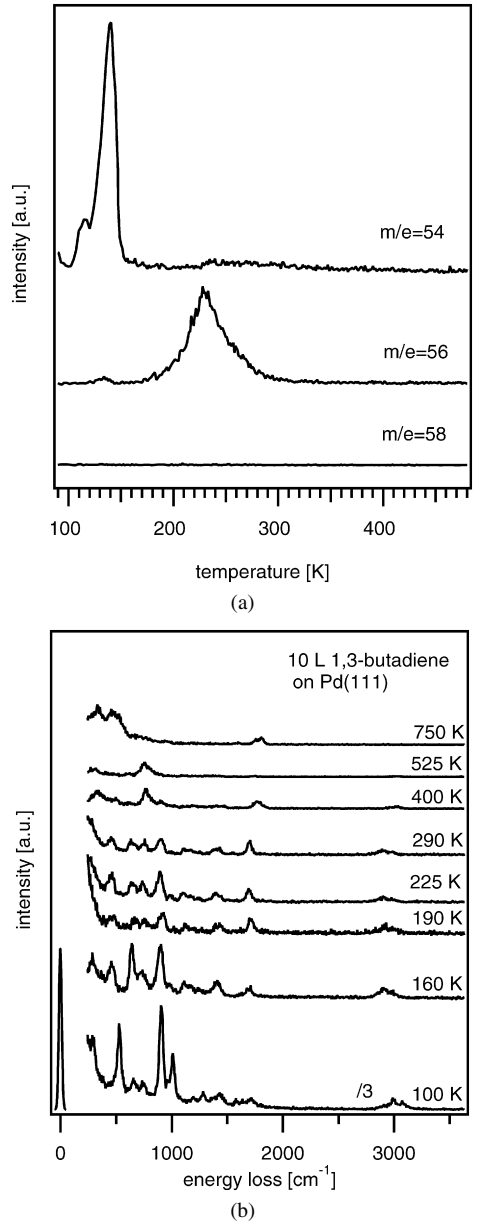

Fig. 1. Top: TPD spectra after adsorption of 4 L H_2 + 6 L butadiene on Pd(111) at 90 K, $\beta = 3$ K/s. Bottom: HREEL spectra series after adsorption of 10 L butadiene at 90 K.

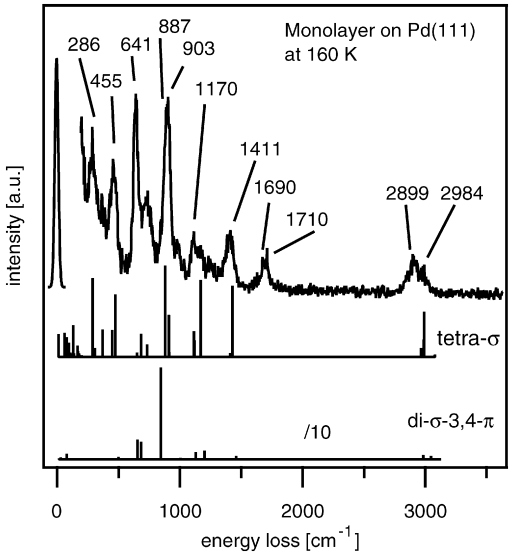

Fig. 2. Experimental monolayer spectrum after adsorption of 10 L butadiene at 90 K and flash to 160 K. Two DFT spectra are shown for tetra-σ and di-σ-3,4-π adsorption modes (1/6 ML coverage).

Table 1
Vibrational mode assignment for butadiene monolayer spectrum on Pd(111) according to calculated spectra

Vibrational mode	Experimental (cm^{-1})	DFT 1/6 ML tetra-σ mode (cm^{-1})
ν(C–H)	2900, 2984	3002
$\delta(CH_2) + \nu$(C–C)	1411	1430, 1415
$\rho(CH_2)$	1170	1170
ρ(CH) + n(C–C)		1123
$\omega(CH_2)$	903	910
$\rho(CH_2)$		879
$\tau(CH_2) + \omega$(CH)	641	653
δ(CCC)		470
ν(C–Pd)	455	451

with the features of the experimental spectrum. Due to the harmonic approach, the ν(C–H) vibrations are overestimated by about 100 cm^{-1}, which is commonly observed. Qualitatively, the tetra-σ adsorption mode is characterized by a downshift of the ν(C–H) vibration to 2903 cm^{-1}, which is typical for sp^3-hybridized carbon atoms and the absence of the ν(C=C) stretching vibration in the range of 1500–1600 cm^{-1}. A detailed vibrational assignment based on the calculated spectrum is given in Table 1. Although the intensities of the calculated di-σ-3,4-π spectrum are very weak, they also fits the experimental spectrum. Therefore, we cannot exclude the possibility that this species coexists as a minority species on the Pd(111) surface, because its adsorption energy is close to that of the tetra-σ species [14]. Only the peak at 1710 cm^{-1} cannot be explained by the calculations. It is not present in the calculated spectra of any of the considered butadiene species, and most likely is due to a carbonylic stretch (C–O) of an unknown species from the residual gas.

Our assignment is at variance with the NEXAFS results from Bertolini et al. [9,10] who proposed a di-σ mode for butadiene on Pd(111) and explained the different selectivities of Pd(111) and Pt(111) by the different adsorption energies on both surfaces. But, as pointed out previously [14], the NEXAFS data also are in agreement with a tetra-σ configuration if a smaller distortion of the butadiene carbon backbone on Pd(111) compared with that on Pt(111) is considered. This is in line with the calculated adsorption geometry of butadiene on Pd(111), which is closer to the gas-phase geometry with the double bonds slightly less activated than on Pt(111). The HREELS spectra available for butadiene on Pt(111) [8,10] look rather different in the fingerprint region compared with our spectrum, giving evidence that the distortion of the molecule is different on both surfaces, thus supporting the NEXAFS data. The downshift of the CH stretching vibration is considered a good measure of the hybridization of a molecule. The ν(CH) vibration is red-shifted

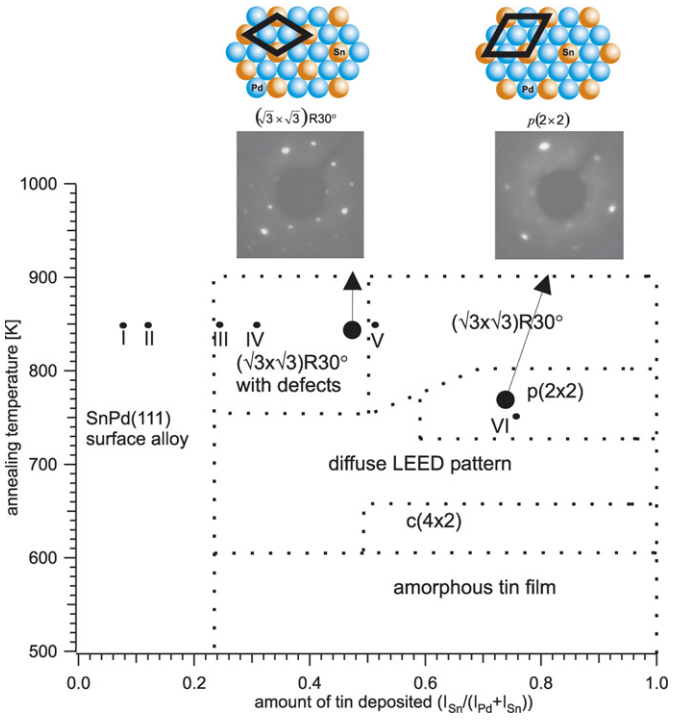

Fig. 3. Phase diagram for PdSn/Pd(111) surface alloys derived from AES and LEED data. On the bottom axis the normalized AES ratios of the evaporated films and on the left axis the annealing temperature are shown.

by 160 cm^{-1} on both surfaces compared with the gas-phase value, indicating similar activation of the double bond. These experimental results agree very well with the theoretical predictions on both systems, suggesting that the selectivity is determined by the differing stability of the transition states on the two surfaces [16]. According to the calculations, butadiene is adsorbed on both surfaces in tetra-σ geometry with similar adsorption energies. The energy gap between the transition states leading to either butene or butane is smaller on Pt(111) than on Pd(111), thus explaining the higher selectivity for butene on Pd.

The data gained from reactions studies under elevated pressure in batch reactors [4–6] have been interpreted mostly in terms of selectivity, which is determined by the relative adsorption energies of butene and butadiene on a surface. If the adsorption energy of butene is small compared with that of butadiene, then butene is displaced by butadiene, suppressing further hydrogenation. Furthermore, readsorption of butene is energetically not favored. But this explanation cannot be applied to UHV conditions, under which readsorption or displacement by gas-phase species cannot occur. The theory of different transition states works much better for these experiments. Compared with data obtained under elevated pressures [7], the selectivity for butene formation is far better under UHV conditions, because butene is immediately desorbs, preventing further hydrogenation.

4. Preparation of the PdSn/Pd(111) surface alloys

PdSn/Pd(111) surface alloys were first reported and characterized by Lee et al. [23]. After evaporating tin films of various thickness, two ordered alloys with either a $(\sqrt{3}\times\sqrt{3})R30^\circ$ or a $p(2\times2)$ superstructure can be prepared by annealing the sample to different temperatures. According to these experiments, tin grows in a Stranski–Krastanov mode, which was verified by our AES experiments. During evaporation, the sample is kept at 200 K to avoid tin diffusion into the bulk. We measured the thickness of the films by the normalized AES intensity $I = I_{Sn}/(I_{Pd} + I_{Sn})$ using the Pd 330 eV and the Sn 433 eV peaks. The completion of a monolayer can be assigned to an intensity ratio of $I = 0.19$. Fig. 3 shows a sketch of a phase diagram derived from AES and LEED data. Above room temperature, tin starts to diffuse into the bulk until at ~1000 K, the Pd (1×1) LEED pattern is observed again, indicating complete dissolution of the tin. TPD experiments indicate that no desorption of tin from the surface occurs. The $(\sqrt{3}\times\sqrt{3})R30^\circ$ superstructure (the thermodynamically most stable one) is produced by annealing to 850 K. For tin films with an AES intensity ratio $I < 0.45$, the alloys contain defects, because the amount of tin is too small to form a surface alloy covering the entire surface. Because the LEED patterns are still very sharp in this region, we suppose that these surfaces consist of $(\sqrt{3}\times\sqrt{3})R30^\circ$ domains and free Pd patches. The $Pd_3Sn/Pd(111)$ surface alloy is produced by annealing tin films with $I > 0.75$ to 750 K. The surface of this $p(2\times2)$ alloy contains less tin than the $(\sqrt{3}\times\sqrt{3})R30^\circ$ structure found for smaller initial Sn deposits, but large quantities of tin are needed in the subsurface region to stabilize the $p(2\times2)$ superstructure [24]. In contrast to both the Pd $(\sqrt{3}\times\sqrt{3})R30^\circ$ alloy and the corresponding PtSn surface alloys, the $p(2\times2)$ alloy is believed to be a multilayer alloy, as can be deduced from UPS [25]. The weak and rather broad LEED spots indicate that the surface does not have good long-range order and that the alloy may contain defect sites. For submonolayer quantities of tin ($I < 0.2$), diluted Sn phases are found that show no order and can be interpreted in terms of a statistical distribution of Sn within the Pd(111) surface.

The adsorption properties of PdSn/Pd(111) surface alloys have been described previously [26] and are similar to those of the corresponding PtSn/Pt(111) alloys. Whereas on top, bridge, and threefold hollow sites are available on the $Pd_3Sn/Pd(111)$ alloy, the latter are not available on $Pd_2Sn/Pd(111)$ alloys. For the monolayer alloys, we estimate the number of available Pd sites (the surface stoichiometry) by measuring the normalized Auger intensities for the annealed alloy surfaces and comparing this with the known stoichiometry of the defect-free $Pd_2Sn/Pd(111)$ surface. The stoichiometries of the first layer of the investigated surface alloys derived from this approach are shown in Fig. 5. The electronic properties of the surface are also changed by alloying with tin. The d-band center of Pd shifts away from the Fermi edge on surfaces with high tin content due to intermixing of Sn and Pd states [27]. In particular, the DOS of the multilayer Pd_3Sn alloy differs from the monolayer alloys, which all have a very similar DOS.

The alloys used in our reaction studies are denoted by Roman numbers for simplicity. Alloys I and II are diluted tin alloys with $I = 0.08$ and $I = 0.12$, and alloys III and IV refer to defect-containing Pd_2Sn alloys with $I = 0.23$ and $I = 0.3$, re-

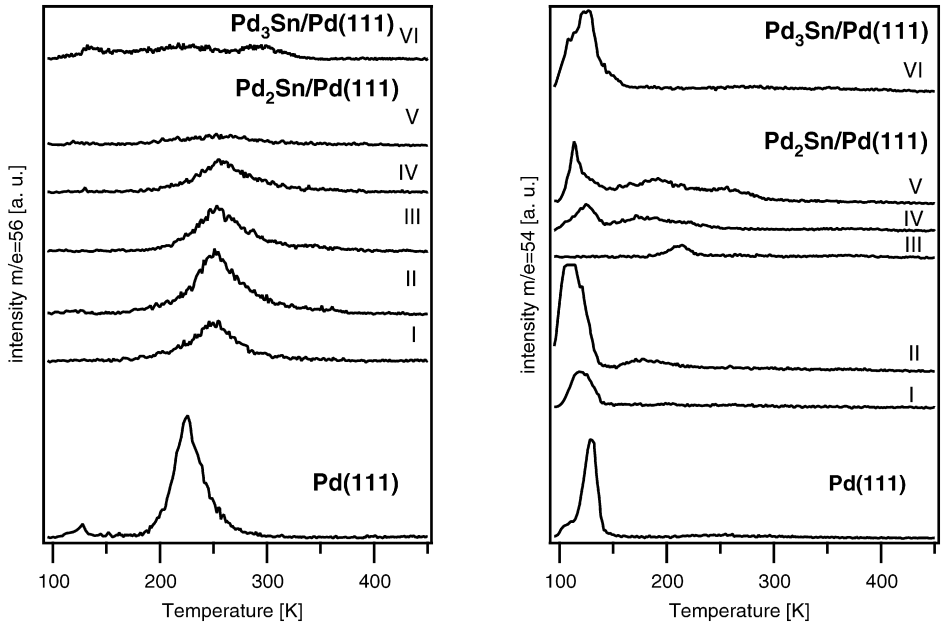

Fig. 4. TPD spectra for $m/e = 54$ and 56 of various PdSn alloys. The roman numbers denote the alloy in the phase diagram Fig. 3. For each spectrum 4 L H_2 + 6 L butadiene were adsorbed at 90 K ($\beta = 3$ K/s).

spectively. Alloy V is a defect-free ordered Pd_2Sn surface alloy ($I = 0.48$), and alloy VI is a Pd_3Sn surface alloy ($I = 0.75$).

5. Hydrogenation of butadiene on PdSn/Pd(111) surface alloys

The reaction studies on the different alloys were conducted by TPD experiments similar to those described above for the bare Pd(111) surface. The TPD spectra for masses $m/e = 54$ for butadiene and $m/e = 56$ for butene are shown in Fig. 4. Besides the butadiene multilayer desorption at 120 K, a monolayer peak at 180 K becomes visible for some of the surface alloys. On the Pd_2Sn alloy (V), the monolayer desorption peak is very broad, with two local maxima at 190 and 250 K, yielding desorption energies (Redhead) of 48 and 64 kJ/mol, respectively. On the monolayer alloys (I–V), butene desorbs at a slightly higher temperature than on Pd(111) in a symmetric peak centered around 250 K. A Redhead approximation yields an activation energy of 64 kJ/mol. On the Pd_3Sn/Pd(111) alloy, butene desorbs in a broad peak ranging from 150 to 300 K with local maxima at 150, 240, and 290 K (activation energies of 37, 61, and 74 kJ/mol). No sign of butane desorption ($m/e = 58$) was detected on any of the surfaces, indicating that hydrogenation produces only mono-hydrogenated butenes.

In contrast to batch reactor studies, deducing quantitative reaction data, such as activity and selectivity, from TPD experiments is not very straightforward. Two main problems must be considered: (i) Deriving absolute quantities from the area under TPD peaks is not a simple matter, and (ii) TPD can detect only species that actually desorb from the surface. Thus, complementary methods, such as AES, photoelectron spectroscopy (PES), and vibrational spectroscopy, which allow quantification of the remaining species on the surface, must be applied. In our study, we have considered four possible reaction pathways: (i) intact desorption of unreacted butadiene from the monolayer, (ii) hydrogenation to either butenes or butane with subsequent desorption, (iii) decomposition of the adsorbed species to smaller hydrocarbon fragments and hydrogen, and (iv) surface carbon formation, which cokes the catalyst.

Quantification of surface carbon is usually be done by either AES or quantification of the total amount of desorbing hydrogen. Both methods fail on Pd(111), because the carbon AES signal at 271 eV overlaps with the Pd signal, and determination of hydrogen desorption is not very exact for Pd, because Pd is an excellent hydrogen storage material. Therefore, we referred to work function measurement using UPS and used the work function change during the reaction as a measure for deposited carbon. A monolayer of hydrocarbons or other adsorbates lowers the work function of transition metal surfaces by ∼1 eV. We assumed a linear relationship between the work function change and surface coverage, which at the least can be considered an approximation to trends in reaction behavior. This method has already been successfully applied by Livneh and Asscher [28], who studied the decomposition of ethene on Ru(001) using work function measurements and found that the work function change during decomposition was linear at lower coverage but reached saturation at high coverage.

To quantify the amount of butene, the TPD corresponding spectra ($m/e = 56$) were integrated in the temperature range 200–300 K. The work function change and butene production data were related to the corresponding quantities found for the bare Pd(111) surface. By applying this method, we avoid the problem of measuring absolute quantities and use relative quantities, making it possible to easily compare the different surfaces. The desorption of unreacted butadiene was measured by integrating the $m/e = 54$ spectra from 160 to 300 K. Because

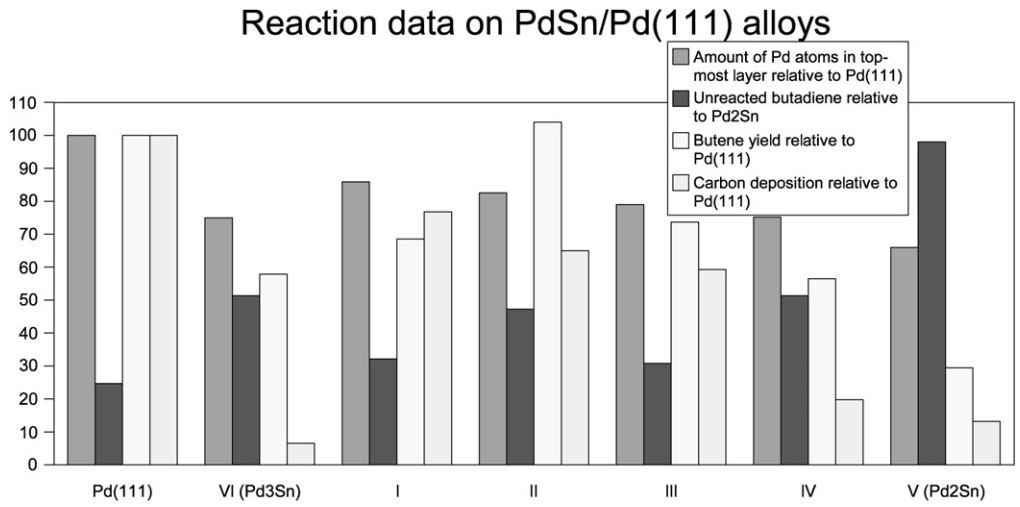

Fig. 5. Compilation of reactivity data for the investigated PdSn/Pd(111) surface alloys. See text for further details.

the Pd_2Sn/Pd(111) surface produced the largest amount of desorbing butadiene, it was used as a reference for this quantity. Fig. 5 compares all relevant quantities.

On alloy I, which shows a statistical distribution of Sn in the surface plane, butene and coke (surface carbon) formation are reduced by approximately the same factor as the number of Pd surface atoms. Pd surface area and coke formation on surface II are very similar to those on surface I, only the butene yield is much higher for this surface. For surfaces III, IV [defect-rich $(\sqrt{3} \times \sqrt{3})R30°$ alloys], and V [defect-free $(\sqrt{3} \times \sqrt{3})R30°$ alloy], the trends for all quantities are nearly linear. With decreasing number of available Pd atoms, butene production and surface carbon deposition are decreasing, and desorption of unreacted butadiene increases. The defect-free Pd_2Sn/Pd(111) surface (V) seems rather unreactive. Butene production is reduced to 30%, and the amount of desorbing butadiene is much higher than on the other surfaces. The alloy IV shows the best compromise between butene production and coke formation of all five monolayer surface alloys (I–V). Butene production is still 56% of the amount found for Pd(111), but the coke formation has dropped to a mere 20%. The multilayer Pd_3Sn/Pd(111) surface (VI) shows a particular behavior, with a rather high Pd content accompanied by a large amount of desorbing unreacted butadiene (50%). The low activity for butadiene hydrogenation is accompanied by a high selectivity toward the formation of butenes. It produces 58% of the butene, but only 6% of the coke, found on bare Pd(111). This behavior is likely caused by the different electronic properties of the Pd_3Sn/Pd(111) multilayer alloy compared with monolayer surface alloys, which are related to a strong decrease in the density of states at the Fermi energy [26] encountered for the Pd_3Sn/Pd(111) alloy.

Only on the well-ordered Pd_2Sn/Pd(111) surface it was possible to obtain good-quality HREELS spectra. A temperature-dependent series is depicted in Fig. 6. Initial inspection of the thermal evolution of the spectra reveals good agreement with the TPD data (Fig. 4). At 100 K, a multilayer spectrum similar to that on Pd(111) is found. After annealing to 160 K, a monolayer spectrum appears, which loses intensity after annealing to 200 and 225 K. Finally, after desorption of the monolayer

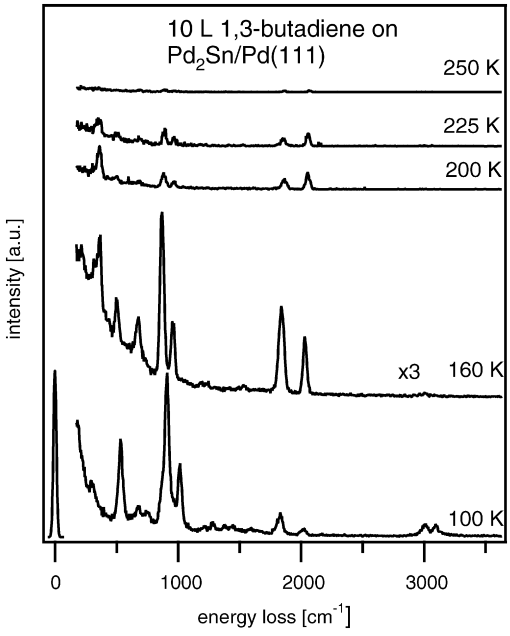

Fig. 6. HREEL spectra series on Pd_2Sn/Pd(111) after adsorption of 10 L butadiene at 90 K.

at 250 K, HREELS indicates a clean surface. Quantitative decomposition of butadiene does not occur, in line with the small amount of coke formed on this surface (see Fig. 5). Fig. 7 shows a magnification of the monolayer spectrum. It is dominated by high-intensity peaks in the fingerprint region (508, 660, and 870 cm^{-1}) and two strong peaks at 1800 and 2050 cm^{-1}, which are attributed to CO adsorbed from the residual gas. The intensity of the ν(CH) vibrations is centered around 3000 cm^{-1}, being red-shifted by 55 cm^{-1} compared with the multilayer spectrum, which is less than on the bare Pd(111) surface. The value of this red shift is indicative for a π-bond, which interacts only weakly with the surface and thus is only slightly activated. The hybridization of the carbon atoms is clearly closer to sp^2 than to sp^3. These findings are also supported by a ν(C=C) vibration at 1560 cm^{-1} that is red-shifted by only 30 cm^{-1} compared with gas-phase data. Table 2 compares the vibration

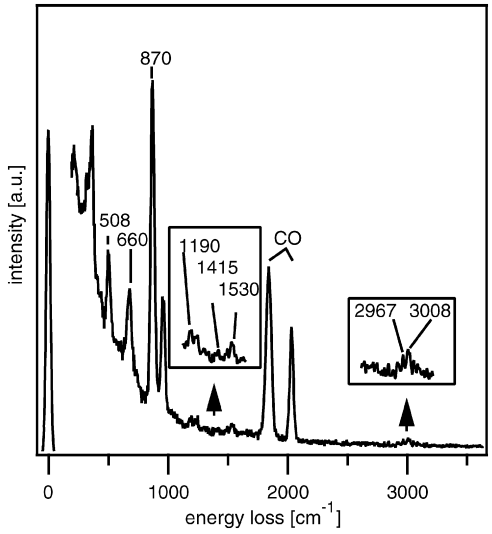

Fig. 7. HREEL spectrum of butadiene monolayer on Pd_2Sn/Pd(111) after adsorption of 10 L butadiene at 90 K and flash to 160 K.

Table 2
Vibrational mode assignment for butadiene monolayer spectrum on Pd_2Sn/Pd(111) in comparison to π-bonded organometallic complexes

Vibrational mode	Pd_2Sn/Pd(111) (cm^{-1})	$Fe(CO)_3C_4H_6$ Ref. [29] (cm^{-1})	$(PdC_4H_6)_n$ Ref. [30] (cm^{-1})
$\omega(CH_2)$	870	896	888
$\omega(CH)$	660	669	
$\nu(C–C)$	1190	1205	1194
$\gamma(CH_2)$	958		
$\delta(CH_2)$ (scissor)	1422	1443	
$\nu(C=C)$	1530	1479	1508, 1618
$\nu(CH) + \nu(CH_2)$	2967, 3008	2920, 3005, 3060	2921, 3009, 3075

energies with the two organometallic complexes $Fe(CO)_3C_4H_6$ and $Pd(C_4H_6)_n$ [29,30]. It is known that butadiene is weakly π-bonded in both cases and the vibration energies of these complexes are very similar to the monolayer spectrum of butadiene on Pd_2Sn/Pd(111). Thus, we conclude that butadiene is bonded more weakly on Pd_2Sn/Pd(111), with a smaller double-bond activation than on Pd(111), leading to a lower reactivity of the molecule.

Taking the previous results for butadiene on PtSn surface alloys on Pt(111) [17,18] into account, we find important similarities to the PdSn surface alloys. Pt_3Sn is more reactive for butene production than Pt_2Sn. Decomposition occurs only on Pt_3Sn, whereas most of the butadiene desorbs unreacted from the Pt_2Sn surface. However, this surface is still more reactive than the corresponding Pd_2Sn surface. When comparing PdSn and PtSn surface alloys, one must keep in mind that the PtSn surface alloys are monolayer alloys, which exhibit nearly the same electronic properties than the Pt(111) surface in UPS [31], whereas the Pd_3Sn alloy is a multilayer alloy with different electronic properties than Pd_2Sn and Pd(111) [26].

For the PtSn systems, vibrational spectra for butadiene do not exist; however, in the surface science approach to catalysis, ethene has been extensively studied as a model molecule for alkenes. The available TPD and HREELS data for ethene on the aforementioned systems exhibit the same trends as those for the more complex molecule butadiene. On Pt(111), Pt_3Sn/Pt(111), and Pt_2Sn/Pt(111), ethene is adsorbed in a di-σ mode, with hybridization shifting closer to sp^2 with increasing tin content and desorption energies of 71, 65, and 49 kJ/mol, respectively [32]. The same trend is visible on the PdSn/Pd(111) surfaces [33] with the hybridization changing from di-σ bonded on Pd(111) to π-bonded on Pd_2Sn/Pd(111) and adsorption energies of 59, 46, and 27 kJ/mol for the three surfaces. Indeed, the behavior of butadiene in terms of adsorption modes and energies follows the same trends as ethene, and both systems show that the catalytic properties of a metal can be improved by alloying it with a second, unreactive metal.

6. Conclusion

We have shown that it is possible to hydrogenate butadiene on Pd(111) under UHV conditions, in marked contrast to Pt(111), for which only decomposition is observed. Because the adsorption on Pd(111) and Pt(111) is of tetra-σ type and the adsorption energies are very similar on the two surfaces, the differences in reactivity/selectivity can be explained only by the surfaces' ability to stabilize different transition states, as has been suggested by theoretical studies.

Quantitative reaction results with TPD are not straightforward, but the general conclusions are that the overall activity of the Pd surface reduces with increasing tin content. The adsorption energy and activation of the double bond (rehybridization of the carbon atoms) also decrease with increasing tin content. These trends follow the same behavior as on PtSn/Pt(111) surfaces and correspond to the model system ethene on PtSn and PdSn. Combining all of these data, we can conclude that butadiene can be hydrogenated to butenes without the formation of butane on all surfaces except Pt(111), on which only decomposition occurs. In contrast, the selectivity of hydrogenation versus decomposition varies over the different alloys. On Pd_3Sn and Pt_3Sn, both reaction pathways are favored, with Pd_3Sn showing good selectivity toward hydrogenation compared with Pd(111) without coking of the catalyst. Pt_2Sn still produces butene with the decomposition pathway suppressed, whereas Pd_2Sn is the most unreactive surface already resembling the behavior of group 11 metals like Cu and Ag, which are poor hydrogenation catalysts but have proven to be powerful in epoxidation reactions.

Acknowledgments

Financial support was provided by the Deutsche Forschungsgemeinschaft (DFG) and the Centre National de la Recherche Scientifique (CNRS) through a binational grant.

References

[1] G.C. Bond, G. Webb, P.B. Wells, G.R. Wilson, J.M. Winterbottom, J. Chem. Soc. (1965) 3218.
[2] P.B. Wells, A.J. Bates, J. Chem. Soc. A (1968) 3064.

[3] J.J. Phillipson, P.B. Wells, G.R. Wilson, J. Chem. Soc. A (1969) 1351.
[4] J. Oudar, S. Pinol, Y. Berthier, J. Catal. 107 (1987) 445.
[5] T. Ouchaib, J. Massadier, A. Renouprez, J. Catal. 119 (1989) 517.
[6] C.M. Pradier, E. Margot, Y. Berthier, J. Oudar, Appl. Catal. 43 (1988) 77.
[7] J. Silvestre-Albero, G. Rupprechter, H.-J. Freund, J. Catal. 235 (2005) 52.
[8] N.R. Avery, N. Sheppard, Proc. R. Soc. London A 405 (1986) 27.
[9] G. Tourillon, A. Cassuto, Y. Jugnet, J. Massadier, J.C. Bertolini, J. Chem. Soc. Faraday Trans. 92 (1996) 4835.
[10] J.C. Bertolini, A. Cassuto, Y. Jugnet, J. Massadier, B. Tardy, G. Tourillon, Surf. Sci. 349 (1996) 88.
[11] S. Katano, S. Ichihara, H. Ogasawara, H. Kato, T. Komeda, M. Kawai, K. Domen, Surf. Sci. 502–503 (2002) 164.
[12] S. Katano, H.S. Kato, M. Kawai, K. Domen, J. Phys. Chem. 107 (2003) 3671.
[13] J. Silvestre-Albero, M. Borasio, G. Rupprechter, H.-J. Freund, Catal. Commun. 8 (2007) 292.
[14] A. Valcárcel, A. Clotet, J.M. Ricart, F. Delbecq, P. Sautet, Surf. Sci. 549 (2004) 121.
[15] F. Mittendorfer, C. Thomazeau, P. Raybaud, H. Toulhoat, J. Phys. Chem. B 107 (2003) 12287.
[16] A. Valcárcel, A. Clotet, J.M. Ricart, F. Delbecq, P. Sautet, J. Phys. Chem. B 109 (2005) 14175.
[17] H. Zhao, B. Koel, Surf. Sci. 572 (2004) 261.
[18] H. Zhao, B. Koel, J. Catal. 234 (2005) 24.
[19] Y. Jugnet, R. Sedrati, J.C. Bertolini, J. Catal. 229 (2005) 252.
[20] E. Nikolla, A. Holewinski, J. Schwank, S. Linic, J. Am. Chem. Soc. 128 (2006) 11354.
[21] C. Dupont, Y. Jugnet, D. Loffreda, J. Am. Chem. Soc. 128 (2006) 9129.
[22] P. Redhead, Vacuum 12 (1962) 203.
[23] A.F. Lee, C.J. Baddeley, M.S. Tikhov, R.M. Lambert, Surf. Sci. 373 (1997) 195.
[24] Y. Teraoka, Surf. Sci. 235 (1990) 245.
[25] J. Breitbach, D. Franke, G. Hamm, C. Becker, K. Wandelt, Surf. Sci. 507–510 (2002) 18.
[26] G. Hamm, T. Schmidt, J. Breitbach, D. Franke, C. Becker, K. Wandelt, Surf. Sci. 562 (2004) 170.
[27] A.F. Lee, R.M. Lambert, Phys. Rev. B 58 (1998) 4156.
[28] T. Livneh, M. Asscher, J. Phys. Chem. B 104 (2000) 3355.
[29] G. Davidson, Inorg. Chim. Acta 4 (1969) 596.
[30] N. Osaka, M. Akita, K. Itoh, J. Phys. Chem. B 102 (1998) 6817.
[31] M.T. Paffet, S.C. Gebhard, R.G. Windham, B.E. Koel, J. Phys. Chem. 94 (1990) 6831.
[32] M.T. Paffet, S.C. Gebhard, R.G. Windham, B.E. Koel, Surf. Sci. 223 (1989) 449.
[33] G. Hamm, Ph.D. thesis, University of Bonn, Germany, 2003, http://hss.ulb.uni-bonn.de/diss_online/math_nat_fak/2002/hamm_guido.